

CrossMark  
click for updatesCite this: *RSC Adv.*, 2016, 6, 95812

# Hydrogels generated by low-molecular-weight PEGylated luteolin and $\alpha$ -cyclodextrin through self-assembly for 5-fluorouracil delivery†

Weixia Qing,<sup>ab</sup> Yong Wang,<sup>a</sup> Huan Li,<sup>a</sup> Jinhua Zhu<sup>a</sup> and Xiuhua Liu<sup>\*ac</sup>

Hydrophobic luteolin (LUT) was conjugated to the oligomeric chain of methoxypoly(ethylene glycol) (mPEG) to form novel amphiphilic mPEG<sub>1900</sub>-LUT conjugates. Then mPEG<sub>1900</sub>-LUT, by using its adjacent 3' and 4' hydroxyl groups, were assembled with magnetic Fe<sub>3</sub>O<sub>4</sub> particles in an aqueous solution to form mPEG<sub>1900</sub>-LUT-Fe<sub>3</sub>O<sub>4</sub> conjugates, which formed hybrid Fe<sub>3</sub>O<sub>4</sub> particles. The spectral properties and micellization of the conjugates were studied. Both mPEG<sub>1900</sub>-LUT and mPEG<sub>1900</sub>-LUT-Fe<sub>3</sub>O<sub>4</sub> conjugates were able to self-assemble into stable supramolecular hydrogels through  $\alpha$ -cyclodextrin ( $\alpha$ -CD) in water, and their gelation times and temperatures were determined. The hydrogels displayed typical porous structures, which are suitable for drug delivery. Therefore, 5-fluorouracil (5-FU) was loaded into the formed hydrogels to control its release *in vitro*. The drug release observations showed that introducing Fe<sub>3</sub>O<sub>4</sub> particles into the hydrogel improved the sustained release effect.

Received 19th August 2016  
Accepted 23rd September 2016

DOI: 10.1039/c6ra20851g

www.rsc.org/advances

## 1. Introduction

Hydrogels have been recently utilized for controlled drug release, because of their excellent hydrophilicity, biocompatibility and low inflammatory response.<sup>1-3</sup> Hydrogels composed of polyrotaxane constitute an important class of remarkable materials that are formed by a linear polymer chain threading through a series of cyclodextrin (CD) cavities.<sup>4-6</sup> Polyrotaxane hydrogels have been reported to be endowed with tunable temperature-responsive potentials. So it is very beneficial to develop effective polyrotaxane hydrogels as delivery systems.<sup>7,8</sup>

Poly(ethylene glycol) (PEG) has also been found to be able to thread through  $\alpha$ -CD molecules of polyrotaxane.<sup>9-12</sup> It has been quite generally stated in the literature that, a high molecular weight (MW > 10k) PEG is necessary for chemical and physical hydrogels. However, water-soluble polymer chains with high molecular weights (normally MW > 10k) are known to be unsuitable for filtration through the human kidney membrane because of their large hydrodynamic radii.<sup>13</sup> Therefore, suitable procedures for preparing hydrogels based on low-MW PEGs and that can be used in pharmaceutical or medicinal applications

are desirable for use as drug delivery and controlled release systems.

Luteolin (LUT, 3',4',5,7-tetrahydroxyflavone) is well known as a flavonoid, which mostly exists in various vegetables, fruits and medicinally important plants. LUT has been shown to display anticancer,<sup>14-17</sup> anti-inflammatory,<sup>18</sup> anti-allergic<sup>19</sup> and anti-amnesic<sup>20</sup> activities. Nevertheless, the application of LUT is hampered, due to its poor solubility.<sup>21</sup>

For the current work, we took into consideration the strong hydrophobicity of LUT to pursue the formation of novel amphiphilic conjugates using LUT as the hydrophobic part of the conjugate. LUT was linked to the terminal group of low-MW (1.9k) methoxy PEG (mPEG) to synthesize novel amphiphilic mPEG-LUT conjugates, which can self-assemble into nanoparticles with a core-shell structure in aqueous solutions. The mPEG-LUT conjugates, due to their having adjacent hydroxyl groups at the 3' and 4' positions, reacted with Fe<sub>3</sub>O<sub>4</sub> particles to form hybrid nanoparticles. It is noteworthy that we succeeded in constructing hydrogels based on the complexes of  $\alpha$ -CD and low-MW mPEG-LUT. At the same time, 5-FU was used as a model drug for investigating the performance of the hydrogels in drug loading and release.

## 2. Materials and methods

### 2.1. Chemicals and materials

LUT and mPEG (MW = 1.9k) were purchased from Sigma-Aldrich. Cesium carbonate, benzyl bromide, 4-toluene sulfonyl chloride and anhydrous dimethyl formamide were purchased from J&K Chemical Technology (Beijing China). All other

<sup>a</sup>Institute of Environmental and Analytical Sciences, College of Chemistry and Chemical Engineering, Henan University, Kaifeng, 475004, P. R. China. E-mail: ll514527@163.com

<sup>b</sup>Medical College, Henan University, Kaifeng, 475004, P. R. China

<sup>c</sup>Key Lab. of Natural Medicine and Immune-engineering of Henan Province, Henan University, Kaifeng, 475004, P. R. China

† Electronic supplementary information (ESI) available. See DOI: 10.1039/c6ra20851g

chemicals were of analytical grade and supplied by Sinopharm Chemical Reagent Co., Ltd (Shanghai, China).

## 2.2. Preparation of Fe<sub>3</sub>O<sub>4</sub> particles

FeCl<sub>3</sub>·6H<sub>2</sub>O, then sodium carboxymethylcellulose (CMC-Na) and finally sodium acetate anhydrous (NaAc) were dissolved in ethylene glycol. The mixture was transferred into a Teflon<sup>TM</sup>-lined autoclave, kept at 200 °C for 10 h and then cooled to room temperature. The solid black products were collected and kept for later use on the basis of ref. 22.

## 2.3. Synthesis of mPEG–LUT conjugates

**Synthesis of 2.** LUT (1) (0.10 g, 0.35 mmol), anhydrous K<sub>2</sub>CO<sub>3</sub> (0.20 g, 1.41 mmol) and KI (0.01 g, 0.07 mmol) were dried under vacuum at 60 °C and then dissolved in dry DMF (5 mL) under a nitrogen atmosphere. After 1 h at room temperature, the reaction mixture was treated with benzyl bromide (0.30 mL, 2.52 mmol) and then heated to 80 °C for 10 h. Deionized water was added into the mixture, and then the mixture was extracted with CH<sub>2</sub>Cl<sub>2</sub> three times. The organic phase was washed with 0.5 mol HCl and saturated brine. The solution was dried with anhydrous MgSO<sub>4</sub>. After the solvent was removed *in vacuo*, the resulting residue was purified by using column chromatography with a silica gel and with CH<sub>2</sub>Cl<sub>2</sub> as the eluent to give the stramineous solid product 2 (0.14 g, 71%). The chemical structure of this product was characterized by analyzing its <sup>1</sup>H-NMR spectrum (Fig. S2†). <sup>1</sup>H NMR (400 MHz, DMSO-*d*<sub>6</sub>): δ 7.734 (d, 1H, *J* = 2 Hz), 7.668 (dd, 1H, *J* = 8.4 Hz, *J* = 2 Hz), 7.309–7.509 (m, 15H), 7.215 (d, 1H, *J* = 8.4 Hz), 7.005 (s, 1H), 6.865 (d, 1H, *J* = 2 Hz), 6.452 (d, 1H, *J* = 2 Hz), 5.260 (s, 2H), 5.236 (s, 2H), 5.220 (s, 2H); MS (ESI, *m/z*): 579.20 [*M* + Na<sup>+</sup>].

**Synthesis of 3.** A solution of 30% NaOH in water (5 mL) and 15 mL of CH<sub>2</sub>Cl<sub>2</sub> was added to mPEG<sub>1900</sub> (1.00 g, 0.53 mmol). The vigorously stirred mixture was dropwise added to a solution of 1.50 g (7.87 mmol) of tosyl chloride in CH<sub>2</sub>Cl<sub>2</sub> (15 mL) over 1 h. The organic layer was then separated and washed with water three times. The volume of CH<sub>2</sub>Cl<sub>2</sub> was reduced by 95% under reduced pressure. The remaining CH<sub>2</sub>Cl<sub>2</sub> was cooled to 0 °C, and 50 mL of anhydrous ether was slowly added to this CH<sub>2</sub>Cl<sub>2</sub> with stirring. After 4 h, compound 3 (0.88 g, 81%) as a white powder was recovered by filtration and washed four times with 100 mL of diethyl ether. The chemical structure of this product was characterized by analyzing its <sup>1</sup>H-NMR spectrum (Fig. S3†). <sup>1</sup>H NMR (400 MHz, CDCl<sub>3</sub>): δ 7.744 (d, 2H, *J* = 8 Hz), 7.296 (d, 2H, *J* = 8 Hz), 4.103 (t, 2H, *J* = 4.8 Hz), 3.765–3.326 (mPEG chain), 2.723 (s, 3H), 2.399 (s, 3H).

**Synthesis of 4.** Compound 2 (0.15 g, 0.26 mmol) and Cs<sub>2</sub>CO<sub>3</sub> (0.34 g, 1.05 mmol) were dissolved in 5 mL of DMF under a nitrogen atmosphere. After 0.5 h at room temperature, compound 3 (0.53 g, 0.26 mmol) dissolved in 5 mL of DMF was added into the compound 2/Cs<sub>2</sub>CO<sub>3</sub>/DMF solution. The resulting mixture was stirred for 20 h at room temperature and then heated to 70 °C for 5 h. Deionized water was added into this mixture, which was then extracted three times with CH<sub>2</sub>Cl<sub>2</sub>. The organic phase was washed with deionized water. The solution was dried with anhydrous MgSO<sub>4</sub>. The filtrate was concentrated

and precipitated in ethyl ether three times at 0 °C. Compound 4 was recovered as a pale yellow powder (0.58 g, 90%). The chemical structure of this product was characterized by analyzing its <sup>1</sup>H-NMR spectrum (Fig. S4†). <sup>1</sup>H NMR (400 MHz, DMSO-*d*<sub>6</sub>): δ 7.690 (s, 1H), 7.628 (d, 1H, *J* = 8.8 Hz), 7.520–7.317 (m, 15H), 7.225 (d, 1H, *J* = 8.8 Hz), 6.971 (s, 1H), 6.733 (s, 1H), 6.619 (s, 1H), 5.275 (s, 2H), 5.253 (s, 2H), 5.247 (s, 2H), 4.168 (t, 2H, *J* = 4.4 Hz), 3.815–3.242 (mPEG chain).

**Synthesis of 5.** A solution of compound 4 (0.57 g, 0.23 mmol) in 50 mL of dry methanol was cooled to 0 °C, and to this mixture we slowly added 5% Pd (0) on activated carbon (0.19 g, 0.03 mmol) under a hydrogen atmosphere. The mixture was stirred overnight, after which it was filtered. The methanol was then evaporated, and the resulting light yellow residue was dissolved in a minimal amount of water and extracted three times with CH<sub>2</sub>Cl<sub>2</sub>. The organic phase was washed with deionized water. The solution was dried with anhydrous MgSO<sub>4</sub>. The filtrate was concentrated and precipitated in ethyl ether three times. Compound 5 was recovered as a pale yellow powder (0.36 g, 72%). The chemical structure of this product was characterized by analyzing its <sup>1</sup>H-NMR spectrum (Fig. S5†). <sup>1</sup>H NMR (400 MHz, DMSO-*d*<sub>6</sub>): δ 10.677 (broad, 1H), 9.683 (broad, 1H), 9.474 (s, 1H), 7.312–7.300 (m, 2H), 6.858 (d, 1H, *J* = 8.8 Hz), 6.489 (d, 1H, *J* = 1.6 Hz), 6.374–6.359 (m, 2H), 4.089 (t, 2H, *J* = 4.4 Hz), 3.803–3.233 (mPEG chain).

## 2.4. Synthesis of mPEG–LUT–Fe<sub>3</sub>O<sub>4</sub> conjugates

A mass of 15 mg of Fe<sub>3</sub>O<sub>4</sub> particles was dispersed completely in 5 mL double-distilled water, to which a volume of 5 mL of the mPEG–LUT solution (4 mg mL<sup>-1</sup>) was then added under sonication for 40 minutes. Then the aqueous phase was separated, freeze-dried, and mPEG–LUT–Fe<sub>3</sub>O<sub>4</sub> was obtained.

## 2.5. Characterizations of the conjugates

The FTIR spectra were recorded on a Thermo Nicolet Avatar 360 spectrometer in transmittance mode using KBr pellets. UV-Vis spectroscopic studies were carried out using a TU-1900 spectrophotometer (Beijing Purkinje General Instrument Co. Ltd.). The saturation magnetization was obtained using an MPMS3 (Quantum Design, US). The zeta potential was recorded using a Malvern Nano-ZS90 instrument at 25 °C.

## 2.6. Preparation of blank and 5-FU loaded hydrogels

One aqueous solution sample of α-CD (80.0 mg mL<sup>-1</sup>) was added to an aqueous solution of mPEG–LUT, and another to mPEG–LUT–Fe<sub>3</sub>O<sub>4</sub>, and for both resulting samples, the concentration was 10 mg mL<sup>-1</sup>. Each composition was mixed thoroughly by sonication for about 2 min followed by incubation at room temperature for 72 h before taking measurements. The gelation times of the supramolecular hydrogels were estimated using a vial-tilting method. The timer was started immediately after mixing the two components and the gelation time recorded was when no flow was observed for at least 1 min. Meanwhile, an α-CD (80.0 mg mL<sup>-1</sup>) solution and 5.0 mg of 5-FU were added to 1.0 mL of an aqueous solution of mPEG–LUT and mPEG–LUT–Fe<sub>3</sub>O<sub>4</sub> (10 mg mL<sup>-1</sup>), respectively. Each

resulting composition was mixed thoroughly by sonication for about 2 min followed by incubation at room temperature for 72 h before measurements were taken.

### 2.7. *In vitro* drug release study

The 5-FU-loaded mPEG-LUT and mPEG-LUT-Fe<sub>3</sub>O<sub>4</sub> supramolecular hydrogels were prepared in respective 1.5 mL reagent bottles. Each reagent bottle was placed upside-down in a dialysis bag with 15 mL of pH 7.4 phosphate-buffered (PBS) solution, which was incubated in 100 mL of PBS at 37 °C with gentle shaking. At predetermined time points, 3 mL of release medium was withdrawn and the same volume of fresh PBS solution was added to maintain a constant volume. The cumulative percentage release (*Q*%) was calculated using the equation

$$Q\% = \frac{C_n \times V_0 + V_i \sum_{i=1}^{n-1} C_i}{m} \times 100$$

where  $C_n$  (mg mL<sup>-1</sup>) is the concentration of drug in the sample,  $V_0$  (mL) is the volume of the release medium,  $V_i$  (mL) is the volume of the replaced medium, and  $m$  (mg) is the mass of the drug in the sample.

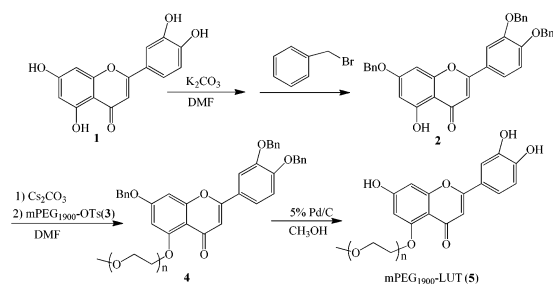
## 3. Results and discussion

### 3.1. Design and synthesis of mPEG-LUT conjugates

The syntheses of mPEG-LUT conjugates are shown in Scheme 1. LUT (**1**) was reacted with benzyl bromide to give **2**, which is a crucial intermediate. During this synthetic process, the experimental results revealed the deprotonation of **1** with K<sub>2</sub>CO<sub>3</sub> (4 equiv.) to be highly selective. Only the proton of the hydroxyl on the 5-position could not be removed. Coupling of **2** with **3** gave **4**, which was deprotected with palladium(0) on carbon to give **5**.

### 3.2. Characterizations of conjugates

Both mPEG-LUT and mPEG-LUT-Fe<sub>3</sub>O<sub>4</sub> conjugates had amphiphilic structures, which were able to self-assemble into stable micelles in aqueous solutions. As shown in Fig. S6,† the average sizes of mPEG-LUT and mPEG-LUT-Fe<sub>3</sub>O<sub>4</sub> conjugate micelles were measured to be about 318.5 nm and 286.9 nm with polydispersity indexes of 0.310 and 0.348, respectively. Furthermore, the micellization of mPEG-LUT was studied by carrying



Scheme 1 Synthetic route of mPEG-LUT conjugates.

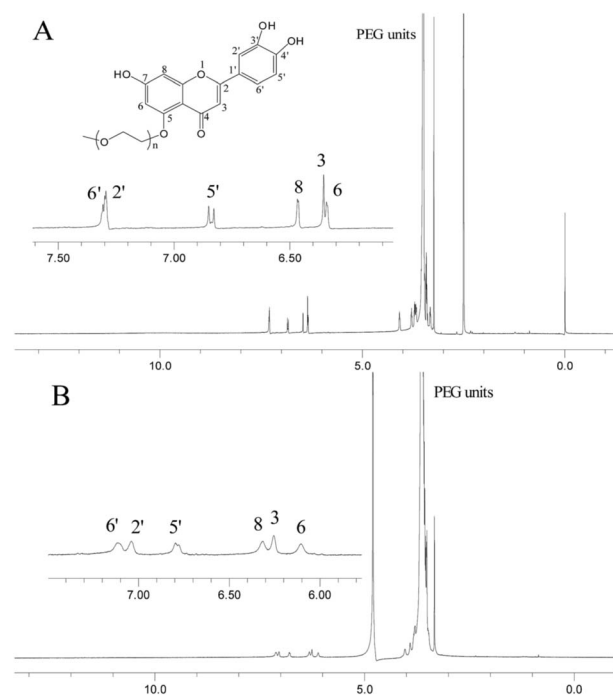


Fig. 1 <sup>1</sup>H NMR spectra of mPEG-LUT in DMSO-*d*<sub>6</sub> (A) and D<sub>2</sub>O (B).

out <sup>1</sup>H-NMR spectroscopy in DMSO-*d*<sub>6</sub> and D<sub>2</sub>O.<sup>23,24</sup> DMSO was used as a non-selective solvent for both mPEG and LUT moieties, whereas water was used as a selective solvent that dissolved the mPEG well but was a poor solvent for LUT. In DMSO, both mPEG and LUT moieties gave rise to sharp peaks, indicative of their rapid molecular motions (Fig. 1A). However, in D<sub>2</sub>O, mPEG moieties gave a sharp peak, but LUT peaks were no longer sharp and were greatly reduced in intensity, indicating the formation of core/shell structures with relatively few LUT segments while the hydrophilic mPEG segments still moved freely in the water (Fig. 1B). The mPEG interacted with water molecules *via* hydrogen bonds, forming an exterior hydrophilic corona extending into the aqueous medium and stabilizing the micelle structure. The results confirmed that mPEG-LUT can self-assemble into a core/shell micelle structure in water.

The FT-IR and UV-Vis spectra of both mPEG-LUT and mPEG-LUT-Fe<sub>3</sub>O<sub>4</sub> conjugates are shown in Fig. 2. As seen Fig. 2A, an Fe-O bending vibration peak of Fe<sub>3</sub>O<sub>4</sub> was observed at about 594 cm<sup>-1</sup> in the spectrum of Fe<sub>3</sub>O<sub>4</sub>, but it shifted to 530 cm<sup>-1</sup> in the spectrum of mPEG-LUT-Fe<sub>3</sub>O<sub>4</sub> because the Fe<sub>3</sub>O<sub>4</sub> reacted with the 3' and 4' adjacent hydroxyls. The Fe-O bending vibration peak of mPEG-LUT-Fe<sub>3</sub>O<sub>4</sub> was very weak because of the low amount of Fe<sub>3</sub>O<sub>4</sub> in the mPEG-LUT-Fe<sub>3</sub>O<sub>4</sub>; only 2.15% of the mPEG-LUT-Fe<sub>3</sub>O<sub>4</sub> consisted of Fe<sub>3</sub>O<sub>4</sub> according to Inductive Coupled Plasma Emission Spectrometer (ICP).

As seen Fig. 2B, the ultraviolet absorption peak of mPEG-LUT at 354 nm sharply shifted to 379 nm after Fe<sub>3</sub>O<sub>4</sub> reacted with the 3' and 4' adjacent hydroxyls. Meanwhile, analysis of the magnetization curves of mPEG-LUT-Fe<sub>3</sub>O<sub>4</sub> conjugates, shown in Fig. 2C, indicated the saturation magnetization value to be about 2.2 emu g<sup>-1</sup>. This value is much smaller than the 80 emu

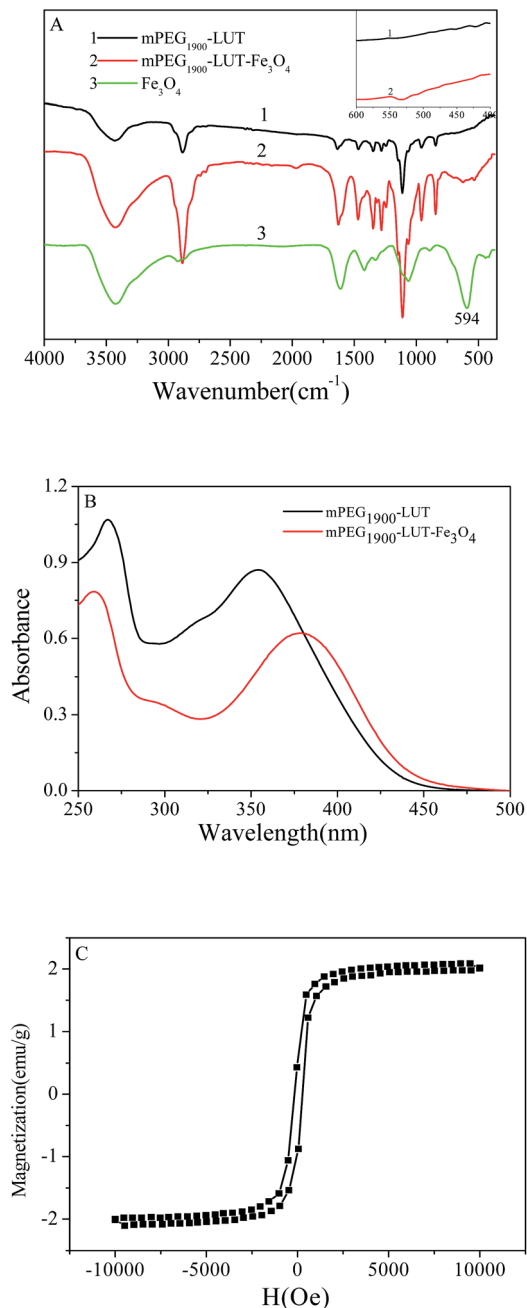
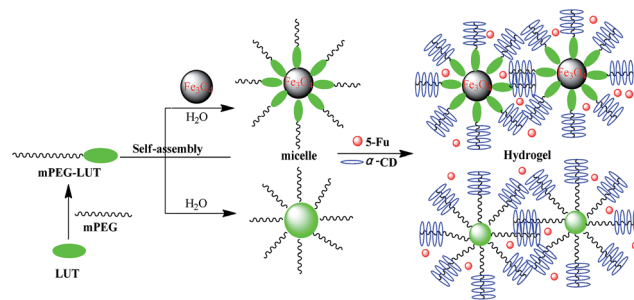


Fig. 2 FT-IR spectra (A) and UV-Vis spectra (B), and magnetization curves (C) of mPEG-LUT-Fe<sub>3</sub>O<sub>4</sub> conjugates.

$g^{-1}$  value for Fe<sub>3</sub>O<sub>4</sub> (see Fig. S1†), and this difference mainly derived from the different amount of Fe<sub>3</sub>O<sub>4</sub> in the mPEG-LUT-Fe<sub>3</sub>O<sub>4</sub> conjugates.

### 3.3. Formation of blank and 5-FU loaded hydrogels

A schematic representation of the supramolecular hydrogels made of mPEG-LUT (or mPEG-LUT-Fe<sub>3</sub>O<sub>4</sub>) conjugates and 5-FU with  $\alpha$ -CD is shown in Scheme 2. Solutions of  $\alpha$ -CD were added to mPEG-LUT and mPEG-LUT-Fe<sub>3</sub>O<sub>4</sub> micelles, respectively, and the resulting compositions were mixed thoroughly by sonication. As expected, homogeneous hydrogels G1 and G2



Scheme 2 Schematic representation of the supramolecular hydrogels made of conjugates and 5-FU with  $\alpha$ -CD.



Fig. 3 Optical photograph of (A) mPEG-LUT/ $\alpha$ -CD sols before being converted to gels, (B) mPEG-LUT/ $\alpha$ -CD supramolecular hydrogels, (C) mPEG-LUT-Fe<sub>3</sub>O<sub>4</sub>/ $\alpha$ -CD sols before being converted to gels, and (D) mPEG-LUT-Fe<sub>3</sub>O<sub>4</sub>/ $\alpha$ -CD supramolecular hydrogels.

gradually formed (Fig. 3). The hydrogels have been shown to be comprised of mPEG/ $\alpha$ -CD complexes.<sup>25,26</sup> Both  $\alpha$ -CD and mPEG-LUT provided the supra-cross-links, which are particularly favorable to the gelation process. Both G1 and G2 exhibited a reversible gel-sol transition with a change in temperature. They started out mobile above a certain temperature, while they returned to an opaque gel phase after cooling to below this temperature. Meanwhile, G1 and G2 were found to be thermo-sensitive at about 40 °C, which is an acceptable temperature for site-specific drug delivery. In addition, introduction of Fe<sub>3</sub>O<sub>4</sub> particles showed remarkable positive effects on gelation time, reducing it from 20 min to 5 min. Perhaps the Fe<sub>3</sub>O<sub>4</sub> particles promoted the gelation process by contributing to the coordination interactions between the metal and polar groups.

The hydrogels were kept for 72 h after formation, and freeze-dried under a vacuum at -54 °C for 24 h. Their morphologies were studied using a JSM-7001F (JEOL Co., Japan), as shown in the images of Fig. 4. G1 and G2 each clearly displayed a typical

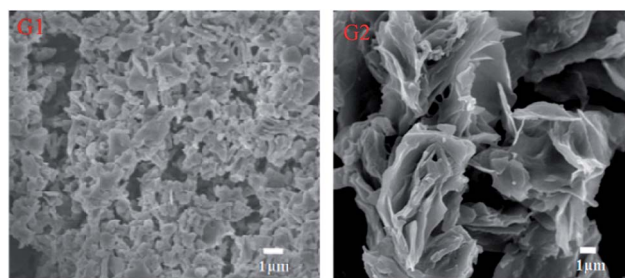


Fig. 4 SEM images of G1 and G2.

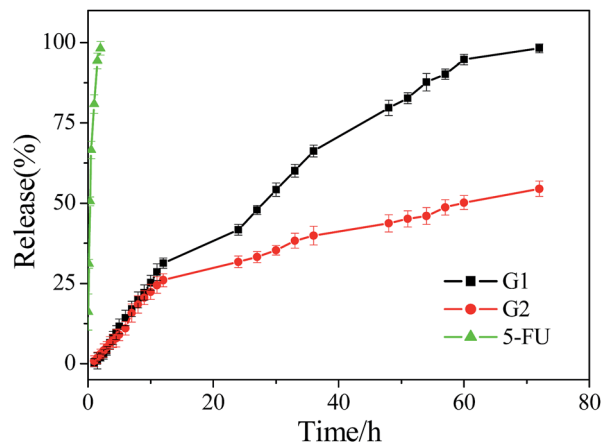


Fig. 5 Release of 5-FU from G1 and G2 in PBS at pH 7.4 and 37 °C.

porous structure. Furthermore, after the introduction of  $\text{Fe}_3\text{O}_4$  particles, G2 showed a flower-like structure, which may have been due to the increase in the network density.

### 3.4. *In vitro* drug release study

As shown in Fig. 5, the hydrogels G1 and G2 loaded with 5-FU showed controlled release properties. The 5-FU content was analyzed by monitoring the UV-Vis peak at a wavelength of 266.4 nm, and the assay method was validated. The calibration curve for 5-FU followed the equation  $A = 0.040 + 48.57C$  ( $R^2 = 0.9991$ ). In general, hydrogel release behavior is mainly influenced by diffusion and the breakup of supra-cross-links. In the current work, the introduction of  $\text{Fe}_3\text{O}_4$  particles yielded a decrease in both the diffusion rate of the encapsulated 5-FU and in the breakup of interchain cross-links, and these decreases may have been due to the small pores and the high network density. The impact of the  $\text{Fe}_3\text{O}_4$  particles was clearly considerable. Meanwhile, sustaining the release of 5-FU was found to be accompanied by releases of G1 and G2. Calculation of the cumulative percentage release of 5-FU allowed the cumulative percentage releases of mPEG-LUT and mPEG-LUT- $\text{Fe}_3\text{O}_4$  to be deduced.

## 4. Conclusions

In conclusion, we have designed and synthesized novel mPEG-LUT and mPEG-LUT- $\text{Fe}_3\text{O}_4$  conjugates, which successfully self-assembled to form hydrogels system with  $\alpha$ -CD. The conjugates displayed typical porous structures, and are hence suitable for drug delivery and tissue growth.<sup>27,28</sup> We successfully developed classical drug-delivery polyrotaxane hydrogels system by introducing  $\text{Fe}_3\text{O}_4$ , which reduced the gelation time. Meanwhile, the formed hydrogels were able to load the anticancer drug 5-FU, and to achieve a targeted release of 5-FU. Such a flexible design provides a new, efficient and mild approach, and this novel system can be applied for the site-specific delivery of drugs using changes in temperature as a trigger.

## Acknowledgements

This work was supported by the Support Plan of Science and Technology Innovation team in Universities and Colleges in Henan Province of China (No. 14IRTSTHN030), Key Project of Science and Technology Research in Education Department of Henan Province in China (No. 14A150011) and Key Technology Research Program of Henan Province in China (No. 152102210257).

## Notes and references

- 1 D. Limón, E. Amirthalingam, M. Rodrigues, L. Halbaut, B. Andrade, M. L. Garduño-Ramírez, D. B. Amabilino, L. Pérez-García and A. C. Calpena, Novel nanostructured supramolecular hydrogels for the topical delivery of anionic drugs, *Eur. J. Pharm. Biopharm.*, 2015, **96**, 421–436.
- 2 X. F. Cheng, Y. Jin, T. B. Sun, R. Qi, H. P. Li and W. H. Fan, An injectable, dual pH and oxidation-responsive supramolecular hydrogel for controlled dual drug delivery, *Colloids Surf., B*, 2016, **141**, 44–52.
- 3 Z. L. Zhang, Z. F. He, R. Liang, Y. Ma, W. J. Huang, R. Jiang, S. Shi, H. Chen and X. Y. Li, Fabrication of a micellar supramolecular hydrogel for ocular drug delivery, *Biomacromolecules*, 2016, **17**, 798–807.
- 4 M. Ceccato, P. L. Nostro and P. Baglioni,  $\alpha$ -Cyclodextrin/polyethylene glycol polyrotaxane: a study of the threading process, *Langmuir*, 1997, **13**, 2436–2439.
- 5 J. Li and X. J. Loh, Cyclodextrin-based supramolecular architectures: syntheses, structures, and applications for drug and gene delivery, *Adv. Drug Delivery Rev.*, 2008, **60**, 1000–1017.
- 6 A. Harada, A. Hashidzume, H. Yamaguchi and Y. Takashima, Polymeric rotaxanes, *Chem. Rev.*, 2009, **109**, 5974–6023.
- 7 H. M. Wang and Z. M. Yang, Molecular hydrogels of hydrophobic compounds: a novel self-delivery system for anti-cancer drugs, *Soft Matter*, 2012, **8**, 2344–2347.
- 8 W. Ha, J. Yu, X. Y. Song, J. Chen and Y. P. Shi, Tunable temperature-responsive supramolecular hydrogels formed by prodrugs as a codelivery system, *ACS Appl. Mater. Interfaces*, 2014, **6**, 10623–10630.
- 9 G. Wenz, B. H. Han and A. Muller, Cyclodextrin Rotaxanes and Polyrotaxanes, *Chem. Rev.*, 2006, **106**, 782–817.
- 10 F. H. Huang and H. W. Gibson, Polypseudorotaxanes and polyrotaxanes, *Prog. Polym. Sci.*, 2005, **30**, 982–1018.
- 11 A. Harada, Preparation and structures of supramolecules between cyclodextrins and polymers, *Coord. Chem. Rev.*, 1996, **148**, 115–133.
- 12 C. Hu and D. D. Kitts, Luteolin and Luteolin-7-*O*-glucoside from Dandelion Flower Suppress iNOS and COX-2 in RAW264.7 Cells, *Mol. Cell. Biochem.*, 2004, **265**, 107–113.
- 13 A. Harada, Design and construction of supramolecular architectures consisting of cyclodextrins and polymers, *Adv. Polym. Sci.*, 1997, **133**, 141–191.
- 14 Q. Zhang, L. Wan, Y. Guo, N. Cheng, W. Cheng, Q. Sun and J. Zhu, Radiosensitization effect of luteolin on human gastric

- cancer SGC-7901 cells, *J. Biol. Regul. Homeostatic Agents*, 2009, **23**, 71–78.
- 15 A. K. Pandurangan, P. Dharmalingam, S. K. Anandasadagopan and S. Ganapasam, Effect of luteolin on the levels of glycoproteins during azoxymethane-induced colon carcinogenesis in mice, *Asian Pacific Journal of Cancer Prevention: APJCP*, 2012, **13**, 1569–1573.
- 16 S. H. Park, H. S. Park, J. H. Lee, G. Y. Chi, G. Y. Kim, S. K. Moon, Y. C. Chang, J. W. Hyun and Y. H. Choi, Induction of endoplasmic reticulum stress-mediated apoptosis and non-canonical autophagy by luteolin in NCI-H460 lung carcinoma cells, *Food Chem. Toxicol.*, 2013, **56**, 100–109.
- 17 Y. Jeon and Y. J. Suh, Synergistic apoptotic effect of celecoxib and luteolin on breast cancer cells, *Oncol. Rep.*, 2013, **29**, 819–825.
- 18 C. Hu and D. D. Kitts, Luteolin and luteolin-7-O-glucoside from dandelion flower suppress iNOS and COX-2 in RAW264.7 cells, *Mol. Cell. Biochem.*, 2004, **265**, 107–113.
- 19 H. Veda, C. Yamazaki and M. Yamazaki, Luteolin as an anti-inflammatory and anti-allergic constituent of *Perilla frutescens*, *Biol. Pharm. Bull.*, 2002, **25**, 1197–1202.
- 20 R. Liu, M. Gao, G. T. Qiang, L. X. Zhang, J. Ying and G. Du, The anti-amnesic effects of luteolin against amyloid  $\beta_{25-35}$  peptide-induced toxicity in mice involve the protection of neurovascular unit, *Neuroscience*, 2009, **162**, 1232–1243.
- 21 K. Shimoia, H. Okadaa, M. Furugoria, T. Godaa, S. Takasea, M. Suzukib, Y. Harab, H. Yamamotoc and N. Kinaea, Intestinal absorption of luteolin and luteolin-7-O- $\beta$ -glucoside in rats and humans, *FEBS Lett.*, 1998, **438**, 220–224.
- 22 R. M. Xing, X. Y. Wang, C. L. Zhang, J. Z. Wang, Y. M. Zhang, Y. Song and Z. J. Guo, Superparamagnetic magnetite nanocrystal clusters as potential magnetic carriers for the delivery of platinum anticancer drugs, *J. Mater. Chem.*, 2011, **21**, 11142–11149.
- 23 C. R. Heald, S. Stolnik, K. S. Kujawinski, C. Dematteis, M. C. Garnett, L. Illum, S. S. Davis, S. C. Purkiss, R. J. Barlow and P. R. Gellert, Poly(lactic acid)-poly(ethylene oxide) (PLA-PEG) nanoparticles: NMR studies of the central solid like PLA core and the liquid PEG corona, *Langmuir*, 2002, **18**, 3669–3675.
- 24 X. B. Xiong, A. Mahmud and H. Uludag, Conjugation of arginine-glycine-aspartic acid peptides to poly(ethylene oxide)-*b*-poly( $\epsilon$ -caprolactone) micelles for enhanced intracellular drug delivery to metastatic tumor cells, *Biomacromolecules*, 2007, **8**, 874–884.
- 25 A. Harada, J. Li and M. Kamachi, Double-stranded inclusion complexes of cyclodextrin threaded on poly(ethylene glycol), *Nature*, 1994, **370**, 126–128.
- 26 A. Harada, Cyclodextrin-Based Molecular Machines, *Acc. Chem. Res.*, 2001, **34**, 456–464.
- 27 V. Gopishetty, I. Tokarev and S. Minko, Biocompatible stimuli-responsive hydrogel porous membranes *via* phase separation of polyvinyl alcohol and Na-alginate intermolecular complex, *J. Mater. Chem.*, 2012, **22**, 19482–19487.
- 28 J. L. He, M. Z. Zhang and P. H. Ni, Rapidly *in situ* forming polyphosphoester-based hydrogels for injectable drug delivery carriers, *Soft Matter*, 2012, **8**, 6033–6038.